Macromolecules

ARTICLE

pubs.acs.org/Macromolecules

Wide-Angle X-ray Diffraction of Cellulose Nanocrystal−Alginate Nanocomposite Fibers

Esteban E. Ureña-Benavides and Christopher L. Kitchens*

Department of Chemical and Biomolecular Engineering, Clemson University, Clemson, South Carolina 29634, United States

ABSTRACT: Wide-angle X-ray diffraction (WAXD) was used to determine the structure and orientation of cellulose nanocrystals (CNC) within alginate nanocomposite fibers and provide correlations with the resulting mechanical property enhancements [Ureña-Benavides et al. Langmuir 2010, 26, 14263]. The alginate junction zones were mostly composed of mannuronate/guluronate (MG) dimers; no evidence was found of an alteration of this structure upon addition of the nanofiller. The orientation of the CNC was studied from the azimuthal intensity distribution of the (2,0,0) reflection. The spread of the orientation increased with higher loads until the nanoparticles within the matrix spiraled around the longitudinal axis, which resulted in a reduction in tenacity and modulus and an increase in elongation at break and toughness. This spiral orientation is also observed in native cellulose fibers and is deterministic of their mechanical properties. Increased fiber stretching during spinning retarded the appearance of a spiral assembly and increased CNC alignment. WAXD was also used as a nondestructive method to measure nanofiller concentration. This work explains unusual mechanical properties observed in CNC−alginate nanocomposite fibers and may be applicable to other nanocomposite systems.

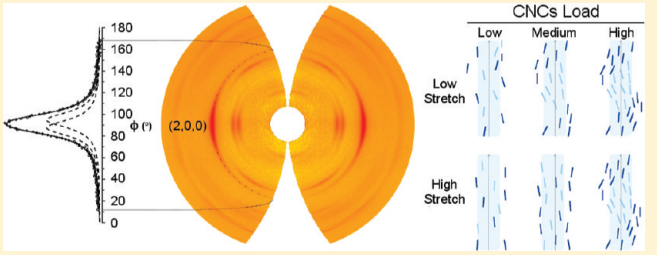

INTRODUCTION

Wide-angle X-ray diffraction (WAXD) is a powerful technique commonly used to describe the crystalline structure of materials. Its applications to polymer composites include the determination of degree of crystallinity, orientation of crystalline regions, concentration of a solid phase, etc., which govern the mechanical properties of the material.[2,3] Increasing the concentration of a stiff material would typically improve the modulus of a composite, and an increase in crystallinity is commonly accompanied by higher alignment and better mechanical performance. However, these trends are not always true, as exemplified in native cellulose fibers. Cotton typically possesses higher degree of crystallinity than ramie, hemp, and flax but has lower tensile strength and modulus. In these cases, the mechanical properties are more strongly impacted by the assembly of the crystallites, which spiral around the fiber axis. Cotton fibers have larger spiral angles than bast fibers like ramie, hemp, and flax. In essence, crystallite orientation defines the mechanical performance of native cellulose fibers.[4,5]

Cellulose nanocrystals (CNC) have recently gained interest as a renewable, environmentally friendly, and cost-effective reinforcing agent for composite materials; however, results vary considerably from one study to another.[6−8] In some instances, the hydrophilic CNC have been found to possess little or no reinforcing effect when introduced into hydrophilic polymer matrices; however, CNC have improved the mechanical performance of hydrophobic materials. Interestingly, the reinforcing capacity for hydrophobic polymers is reduced if the CNC are surface modified to make them hydrophobic.[9,10] The processing techniques, particle−matrix interactions, and particle−particle interactions significantly impact the reinforcing capabilities of CNC and are important factors to take into account.[8]

In a recent paper, we reported a reduction of tenacity and tensile modulus of calcium alginate fibers with the addition of CNC. However, small concentrations of the nanoparticles increased the elongation at break and enabled a nearly 2-fold increase in apparent jet stretch (J_A), ultimately forming stronger fibers (J_A is defined as the tangential velocity of the first roller divided by the linear extrusion velocity).[1] The addition of CNC had a significant impact on the structure of the nanocomposite fiber and thus is the focus of this study.

Calcium alginate fibers are formed by electrostatic cross-linking of polymer chains via divalent Ca ions; their mechanical performance is primarily dependent on the type and strength of the junction zones.[11] We had hypothesized that the CNC interfered with the formation of junction zones, thus disrupting the "egg box" structure and causing a detriment of mechanical properties. However, since increased fiber stretching ultimately led to stronger fibers, it was also believed that the orientation within the fibers played a fundamental role.

In this study, we obtained WAXD profiles of CNC−calcium alginate fibers spun at different J_A and variable cellulose loads. The diffraction patterns were used to study the effects of CNC and processing conditions on the alginate structure and CNC orientation. For this purposes a deconvolution of the profiles was achieved, and individual patterns were obtained for alginate and

Received: November 30, 2010
Revised: February 22, 2011
Published: April 08, 2011

cellulose as separate phases. The degree of orientation and assembly of the cellulose crystallites were quantified by analyzing the intensity distribution of the (2,0,0) reflection. The same signal was used to obtain a calibration curve for the nanocrystals concentration.

EXPERIMENTAL SECTION

Materials. Alginate fibers were formed using high-viscosity sodium alginate with a purity of 98.4%, as purchased from MP Biomedicals, LLC (catalog number 154723). The alginate was isolated by the manufacturer from the seaweed *Macrocystis pyrifera* (kelp). Alginates isolated from the same seaweed have similar chemical compositions—61.0% mannuronate (M) and 39.0% guluronate (G)—with fractions of MM, GG, and MG blocks ranging from 0.38 to 0.43, 0.16 to 0.21, and 0.36 to 0.46, respectively.[11−13] It must be noted that a relatively low concentration of G blocks is present for this source of alginate. CNC were isolated from Whatman cellulose filter aid. Sulfuric acid (98%) was purchased and diluted to 64%. Technical grade anhydrous calcium chloride was used for fiber coagulation, and ACS grade acetone was employed for fiber dehydration.

Isolation of Cellulose Nanocrystals. The isolation of the CNC was achieved by acid hydrolysis of cotton cellulose (Whatman filter aid) with 64 wt % sulfuric acid at 45 °C for 50 min. The reaction was quenched with cold deionized water, and then the CNC were purified through precipitation, decantation, and dialysis. More details regarding this procedure can be found elsewhere.[1,14−16]

Preparation of CNC−Alginate Fiber Nanocomposites. The calcium alginate fibers filled with CNC were prepared by wet spinning an aqueous suspension of the CNC and sodium alginate into a 5 wt % $CaCl_2$ coagulating bath. Fibers with CNC loads of 2.0, 5.0, 10, 25, and 50 wt % were prepared. The spinning dopes had different stretching capacities depending on cellulose concentration; thus, the apparent jet stretch was varied from 2.0 to 4.6 depending on the CNC content. The maximum J_A that can be obtained at a specific CNC load was considered to be 0.2 units below the value at which one or more filaments broke during fiber spinning. More details regarding fiber spinning can be found elsewhere.[1]

Collection of WAXD Data. The fibers were glued to a small tab (5 × 1 cm) made of cardboard file folder with a hole in the center (1 × 0.5 cm) which was aligned with the specimen. Caution was taken to ensure that the yarns were all straight and parallel to each other. The glue was only applied to the ends of the samples to avoid interaction with the beam. The specimen was then fixed to a goniometer head and aligned with the beam to allow the X-rays to pass through the fibers. The Cu Kα_1 X-ray beam had a wavelength (λ) of 0.154 nm and a 0.5 mm diameter at the sample position. The WAXD patterns were recorded on a Fujifilm BAS-IP MS2325 image plate (IP), which was located 112 mm from the sample. The IP was then scanned with a Fujifilm BAS-1800 II scanner to transform the data into an electronic format.

The patterns were corrected for air scattering and cosmic background. This correction was achieved by collecting a diffraction pattern without any sample and subtracting it from the raw data. A Fraser correction was performed to convert the blackening densities and pixel positions to intensities and reciprocal space coordinates.[17]

Extraction of One-Dimensional Diffraction Patterns. The intensity at each 2θ, which is twice the Bragg angle, was averaged with respect to the azimuthal angle (ϕ) to obtain a one-dimensional, powder-like, diffraction pattern for each sample. To account for variations in the intensity of the diffracted beam and exposure time, all data were normalized to the intensity at $2\theta = 54°$, averaged from an equatorial slice ($67° < \phi < 113°$) of the same pattern. This position was chosen because no reflections from cellulose or alginate were observed at that Bragg angle and because the experimental setup did not allow for measuring the intensity at $2\theta = 0°$. The diffraction patterns were divided into two sections ($9.0° < 2\theta < 19.6°$ and $18.0° < 2\theta < 26.6°$), and the cellulose and alginate peaks were deconvoluted in each section by fitting the profile to multiple Lorentzian peaks. During fitting, the center position of each peak was constrained to ±1° of a visual estimate, while for the amorphous halo this range was ±4°; the width and area in all cases were forced to positive values. The signals corresponding to cellulose and alginate were then joined to obtain a complete diffraction pattern for each component of the fiber.

CNC Orientation. From the 2D pattern, a distribution of the intensity (I) with respect to ϕ was obtained by scanning along the arc defined by $2\theta = 22.9°$, which corresponds to the (2,0,0) reflections of the cellulose Iβ crystals.[18] The measured $I(\phi)$ is a convolution of the orientation distribution and instrumental broadening; however, the width of the instrumental profile was considered negligible for which $I(\phi)$ was attributed entirely to the orientation of the CNC. $I(\phi)$ for the (2,0,0) reflection was used to quantify the degree of orientation of the nanocrystals within the fiber. For this purpose $I(\phi)$ was fit to a Lorentzian distribution and the full width at half-maximum (fwhm), which has an inverse relation with alignment, was measured for each of the samples.

Alternatively, an order parameter (S) was calculated from $I(\phi)$ using the procedure described by Alexander.[19] This method calculates the second moment of the orientation distribution function (P_2)

$$S = P_2(\cos \phi_{c,z}) = \frac{1}{2}(3\langle \cos^2 \phi_{c,z}\rangle - 1) \quad (1)$$

where $\phi_{c,z}$ is the angle formed between the c axis of the cellulose unit cell and the fiber axis. It was necessary to first calculate $\langle \cos^2 \phi_{200,z}\rangle$ from $I(\phi)$ by eq 2:

$$\langle \cos^2 \phi_{200,z}\rangle = \frac{\int_0^{\pi} I(\phi) \sin \phi \cos^2 \phi \, d\phi}{\int_0^{\pi} I(\phi) \sin \phi \, d\phi} \quad (2)$$

where $\phi_{200,z}$ is the angle between the (2,0,0) planes and the fiber axis. The integrals were solved numerically for each sample, and $\langle \cos^2 \phi_{c,z}\rangle$ was determined using eq 3

$$\langle \cos^2 \phi_{c,z}\rangle = 1 - 2\langle \cos^2 \phi_{200,z}\rangle \quad (3)$$

which is true for a set of monoclinic crystals with fiber symmetry. This quantity can be introduced into eq 1 to obtain the order parameter.

RESULTS AND DISCUSSION

Calcium Alginate Structure. WAXD measurements were first performed on calcium alginate fibers without CNC; the respective diffraction pattern is shown in Figure 1 with the fiber axis in the vertical direction. The broad halos indicate that the sample has low crystallinity, but there are a few sharp reflections at meridional and near-meridional positions. The most distinctive of these is observed at $2\theta = 9.7°$, which corresponds to a d-spacing, $d = \lambda/(2 \sin \theta)$, of 0.91 nm. Other weaker and broader reflections are found at 2θ values of 12.2°, 19.1°, and 21.3°, which are attributed to d-spacings of 0.73, 0.46, and 0.42 nm.

The structure of the junction zones in alginate gels is commonly described by the well-known "egg-box" model. According to this model, the GG blocks in the alginate chains assemble in a zigzag manner and enclose the divalent calcium cations in a structure that resembles an egg box. It has been suggested that the MG blocks also take part of the junction zones in calcium alginate gels forming a similar structure.[20] Our measurements support this hypothesis by the presence of a strong and sharp meridional reflection at a d-spacing of 0.91 nm. This signal is

attributed to (0,0,1) planes of MG dimers, representing the *c* lattice parameter (fiber direction) of an MG unit cell (Figure2). In the case of a GG dimer this distance would be 0.87 nm, as predicted by the egg-box model (Figure 2).

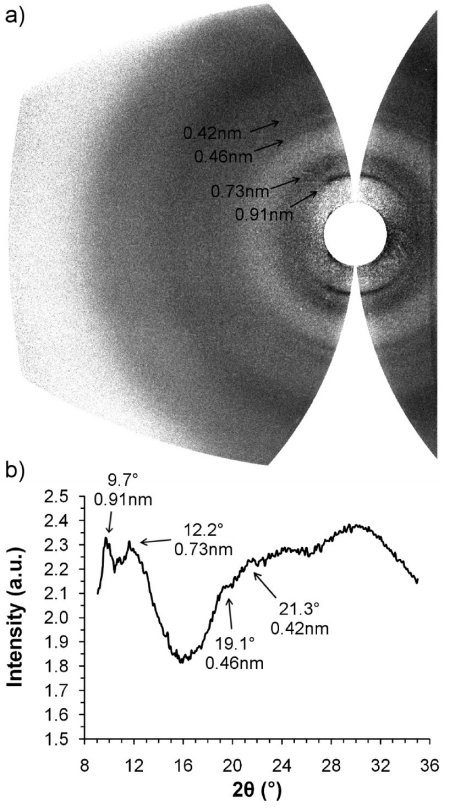

Figure 1. WAXD of a calcium alginate fiber spun at a J_A of 2.4. (a) Two-dimensional fiber diffraction pattern with the fiber axis in the vertical direction; the image contrast was enhanced for clarity. (b) One-dimensional "powder" diffraction pattern obtained from integrating the unenhanced two-dimensional scattering.

Most of the sharp signals come from meridional positions, and virtually no equatorial reflections other than broad halos were observed, indicating that long-range order is present along the fiber axis but not in the radial direction. Thus, an ordered array of several dimers is unlikely. It is possible that the poor lateral order enables the presence of the (0,0,1) signal. Lateral chain packing may require the presence of an additional diffracting layer at exactly one-half the *c*-axis, which would cause destructive interference of X-rays diffracted at the respective Bragg angle.[21]

The WAXD data did not show the presence of GG blocks in the junction zones. The G content of the alginate used in this study is low; it is possible that the few reflections from GG blocks in the junction zones are buried inside the broad amorphous halos. It is thus assumed that most of the strength of the fibers is product of the interaction between MG blocks.

Effect of CNC on Calcium Alginate Structure. The CNC−alginate fiber diffraction patterns may be regarded as a convolution of a calcium alginate component and a CNC component. Reflections from both, calcium alginate and CNC, can be observed in the 2D profile in Figure 3a. The 1D "powder" diffraction pattern in Figure 3b was deconvoluted by fitting all the peaks and assigning each of them to alginate or cellulose, thus obtaining individual traces for each component. The fitted profile, which represents the addition of the alginate and CNC components, describes very accurately the shape of the experimentally measured trace. This separation was performed for all fibers, and the results are shown in Figures 4 and 5.

In our previous work, we determined that addition of CNC caused a decrease in the tenacity and modulus of the fibers when the processing conditions were kept constant.[1] Two possible explanations were suggested: the cellulose crystals disrupted the order in the alginate junction zones, or they reduced the degree of alignment within the fibers. Disorder of the junction zones would cause broadening and a reduced intensity of the alginate signals, especially at 9.7°, which is not the case presented in Figure 4. Instead, the peak at 19.1° become sharper and more intense; thus, the CNC appear to induce ordering of the calcium alginate chains. Previously, we reported that the presence of

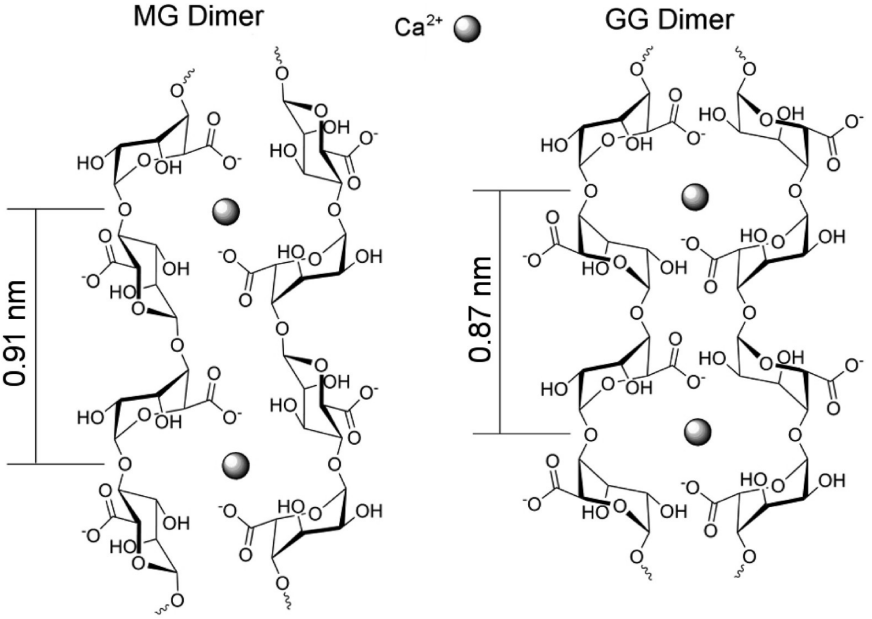

Figure 2. Schematic structure of MG and GG dimers in the junction zones of calcium alginate fibers.

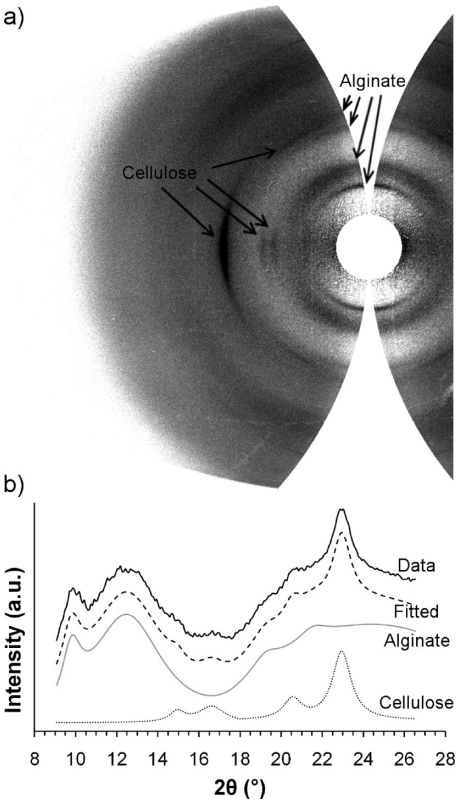

Figure 3. WAXD of a 10 wt % CNC−calcium alginate fiber spun at a J_A of 2.4. (a) Contrast enhanced 2D diffraction pattern with the fiber axis in the vertical direction. (b) Deconvolution of the alginate and CNC components of the powder diffraction pattern; curves are offset for clarity.

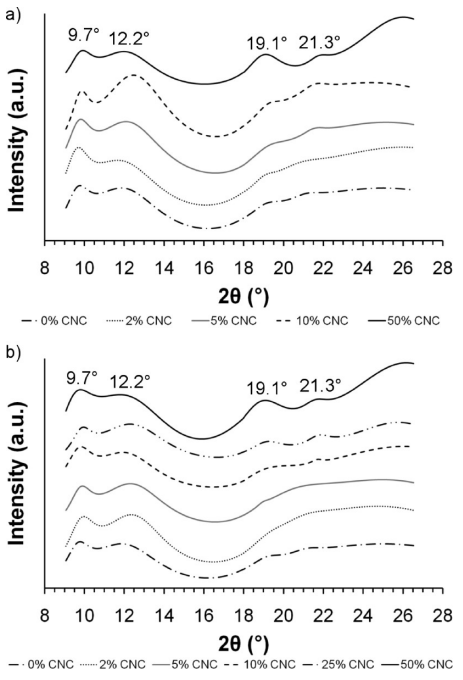

Figure 4. "Powder" diffraction pattern of the calcium alginate component: (a) traces for fibers spun at a constant J_A of 2.4; (b) traces for the fibers spun at the maximum J_A for the specific CNC load. The peak positions represent the average of all the traces.

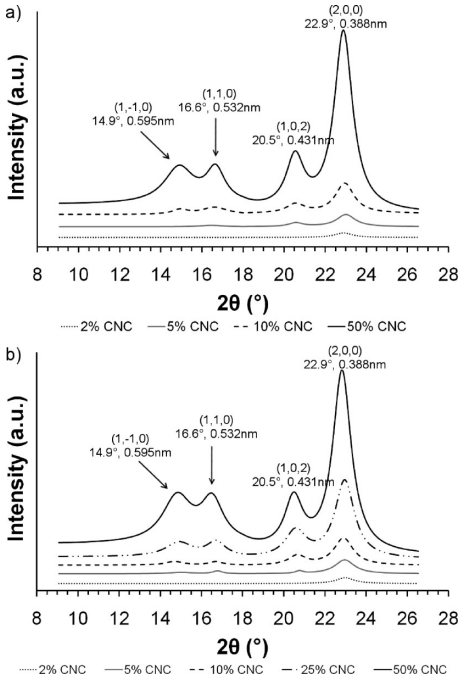

Figure 5. "Powder" diffraction pattern of the CNC component: (a) traces for fibers spun at a constant J_A of 2.4; (b) traces for the fibers spun at the maximum possible J_A for the specific CNC load. The peak positions represent the average of all the traces.

CNC in a sodium alginate aqueous solution induced the formation of a liquid crystalline phase; this is also an indication that the nanoparticles are templates for alginate orientation.[1] Thus, the detriment of the fibers mechanical properties cannot be attributed to a breakdown of the alginate structure.

The alginate traces may be regarded as a "background" for the CNC diffraction patterns, especially at large cellulose concentrations. The CNC traces extracted from the different fibers are shown in Figure 5; they describe the intensity that stands above the alginate profiles. A simulated powder diffraction pattern was obtained based on the cellulose Iβ structure determined by Nishiyama et al.;[18] the results showed four main peaks and a coincidence in d-spacings within $\pm$0.001 nm of the measured averages. This supports the method used for separating the component profiles as well as confirms the structure and crystalline nature of the nanoparticles.

Nanoparticles Orientation. The strongest cellulose peak is located at 22.9° and corresponds to reflections from the (2,0,0) planes. Its intensity is measurable even at 2 wt %, while the other peaks are hardly distinguishable at 5 wt %. The intensity distribution $I(\phi)$ along the (2,0,0) arc in the 2D pattern was used to quantify the alignment of the nanocrystals. A sharp distribution indicates high degree of alignment, while a broad peak represents the opposite. The fwhm of $I(\phi)$ was measured by fitting the data to Lorentzian curves, and the order parameter was calculated directly from the experimental data using eqs 1−3. The results are shown in Figure 6 (1/fwhm is plotted for comparison with the order parameter). Both methods show the same trend: a higher degree of CNC alignment for small CNC loads and high jet stretches. These results confirm our hypothesis that the degree of orientation of the nanocrystals is the main cause of the weakening of the alginate fibers upon addition of CNC at constant J_A and the subsequent

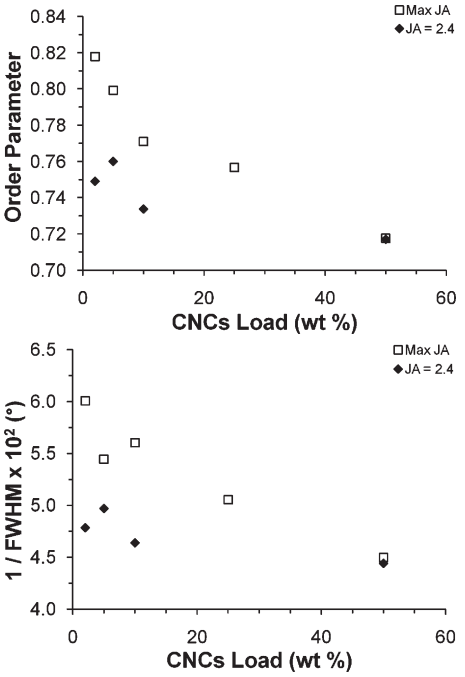

Figure 6. Effect of CNC load on the degree of orientation of the crystallites, expressed as order parameter (top) and the inverse of the full width at half-maximum of $I(\phi)$ (bottom). Maximum J_A's are 2.4, 3.4, 3.8, 4.2, 4.6, and 2.8 for 0, 2, 5, 10, 25, and 50 wt % loads, respectively.

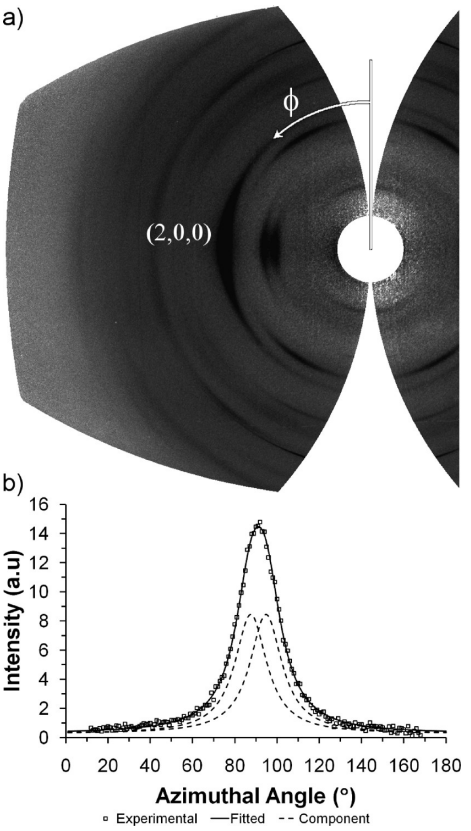

Figure 7. Azimuthal intensity scan of the (2,0,0) cellulose reflection. (a) 2D diffraction pattern of a 50 wt % CNC−calcium alginate fiber spun at a J_A of 2.4. (b) Intensity profile resolved into two equal Lorentzian distributions.

reinforcement at maximum J_A.[1] It could be expected that the tenacity and modulus of the nanocomposites would continue to decrease, accompanied by an increment in toughness, as the CNC load is increased to 50 wt % or more, given that the degree of orientation also continues to diminish. However, when the cellulose concentration reaches a percolation threshold, the particles form an interconnected network that reinforces the composite.[8,22]

In native cellulose fibers (e.g., cotton, compression wood, etc.), the crystallites assemble in a spiral around the longitudinal axis of the fiber.[5,23] It is conceivable that the CNC in the composite fibers may also tend to order in a similar fashion as the load is increased. To analyze this, the azimuthal intensity profile can be resolved into two equal peaks that are separated by twice the spiral angle (ψ).[23,24] The profiles of all the fibers were fit to two Lorentzian peaks of equal widths (w_i) and areas, with center positions separated by 2ψ. As an example, Figure 7 shows the resolved $I(\phi)$ of the (2,0,0) cellulose reflection of a fiber containing 50 wt % CNC; the component peaks are located at 86.4° and 93.6° each, while the convoluted peak is centered at 90°. Table 1 presents the measured spiral angles and peak widths for the fibers as well as the tensile properties;[1] interestingly, the appearance of a spiral angle coincides with a decrease in the tenacity and modulus of the fibers. At a constant J_A of 2.4, the reduction in modulus happens just before the appearance of the spiral at 2 wt % CNC, which is consistent with the large w_i measured by WAXD. It must also be noted that the toughness was generally large for fibers with low degree of alignment, at small J_A, but also low CNC concentration.

The Lorentzian peak width, w_i, is proportional to the spread of crystallite orientations around a preferred direction, which is the fiber axis when the spiral is absent. However, this direction is tilted by the angle ψ if a spiral is formed. A trend is observed where w_i increases with increasing CNC content; however, a step decrease is observed upon appearance of the spiral. The data suggest that increasing the CNC load causes the crystallites to twist away from the longitudinal axis of the fiber, until a more stable, spiral-like, assembly is formed. When the cellulose concentration continues to increase, the spread around the preferred (tilted) orientation also increases. It is hypothesized that at even higher CNC concentrations, the spiral angle and w_i will get larger up to some unknown maximum value for a pure cellulose fiber. A schematic representation of this assembly can be observed in Figure 8.

The nature of the cellulose crystallites is to twist with respect to each other. This is evidenced by the formation of chiral nematic aqueous suspensions of CNC[15] and the spiral assembly of the crystallites in native cellulose fibers.[23] This assembly may be caused by the structure of the individual crystallites; recently, Elazzouzi-Hafraoui et al. observed that micrometer long CNC isolated from tunicate twist themselves, forming a ribbonlike geometry. They suggest that nanosized CNC, like those isolated from cotton, possess the same twist, but it is not easily detected because the half-helical pitch is larger than the crystallites themselves (1.2−1.6 μm).[25] During spinning of CNC−calcium alginate fibers, the extensional flow field forces the nanoparticles to align parallel to the fiber axis, but as the crystallites concentration increases, the particle−particle interactions strengthen and compete with the external forces, leading to the structures described in Figure 8. It must be noted that at maximum J_A the spiral appears at higher CNC concentrations; this is because the

Table 1. Comparison of Tensile Properties with the Spiral Angles and Component Peak Widths of the Cellulose (2,0,0) Intensity Distribution in CNC−Calcium Alginate Fibers[a]

	at J_A = 2.4					at max J_A				
CNC load (wt %)	spiral angle ψ (deg)	width w_i (deg)	tenacity × 10^2 (gpd)	modulus (gpd)	toughness × 10^2 (gpd)	spiral angle ψ (deg)	width w_i (deg)	tenacity × 10^2 (gpd)	modulus (gpd)	toughness × 10^2 (gpd)
0			14.9 ± 0.4	3.1 ± 0.1	3.3 ± 0.2			14.9 ± 0.4	3.1 ± 0.1	3.3 ± 0.2
2	0	21 ± 5	15.2 ± 0.5	2.6 ± 0.1	3.9 ± 0.1	0	17 ± 3	18.0 ± 0.7	3.8 ± 0.2	3.6 ± 0.2
5	3.6 ± 0.8	15 ± 2	14.4 ± 0.3	2.8 ± 0.1	3.7 ± 0.1	0	18 ± 1	18.7 ± 0.5	5.5 ± 0.1	2.4 ± 0.1
10	3.8 ± 0.5	16 ± 2	12.9 ± 0.3	2.5 ± 0.1	3.0 ± 0.1	0	17.8 ± 0.6	20.6 ± 0.7	6.9 ± 0.2	2.5 ± 0.1
25						3.0 ± 0.2	16.6 ± 0.5	16.4 ± 0.6	6.2 ± 0.2	1.6 ± 0.1
50	3.6 ± 0.2	18.4 ± 0.3	17.8 ± 0.4	6.8 ± 0.2	2.4 ± 0.1	3.2 ± 0.2	19.1 ± 0.4	16.4 ± 0.5	6.9 ± 0.2	1.8 ± 0.1

[a] Maximum J_A's are 2.4, 3.4, 3.8, 4.2, 4.6, and 2.8 for 0, 2, 5, 10, 25, and 50 wt % loads, respectively.

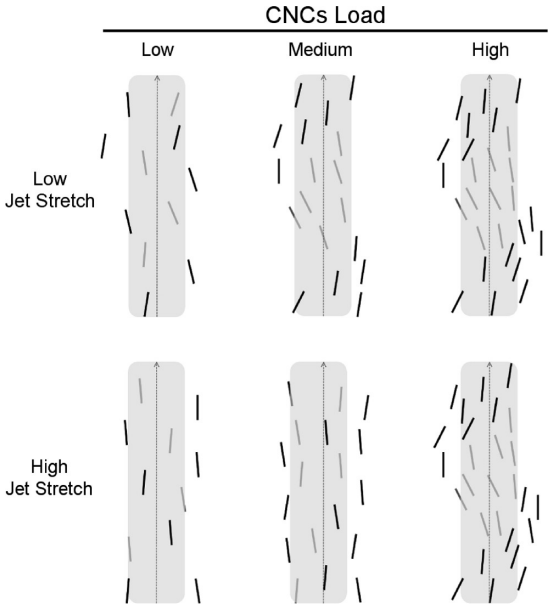

Figure 8. Schematic representation of the assembly of CNC in a calcium alginate fiber. The nanocrystals are incorporated within the alginate matrix and spiral around the fiber axis as the load is increased. The angle of the spiral was exaggerated for illustrative purposes.

larger elongation rate amplifies the external force field, thus requiring a larger CNC load to exceed the extensional forces. Given the good chemical compatibility between the CNC and the alginate matrix, this assembly may be transferred to the alginate chains with CNC acting as a structure-directing agent.

It is worth noting that the same relationship observed here between CNC assembly and mechanical performance is observed in natural cellulose fibers. Highly aligned bast fibers, where the crystallites show small spiral angles (e.g., hemp, flax, ramie, etc.), possess higher tensile strength and elastic modulus and smaller elongation at break than cotton fibers which have large spiral angles and low alignment.[4,5] This opens a variety of opportunities for the industrial production of cellulose based fibers with a wide range of mechanical properties that can be tuned by modifying simple processing conditions such as jet stretch or draw ratio.

Nanoparticles Load. In Figure 5, it was possible to observe that the strongest cellulose peak has a measurable intensity even at 2 wt % CNC. This strong signal may be used to obtain a

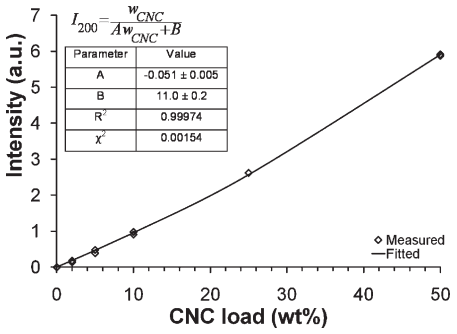

Figure 9. CNC load calibration curve showing experimental values as well as the fitted curve.

calibration curve for the nanoparticles load. The expression

$$I_{200} = I_{200}^{0}\frac{w_{CNC}(\mu/\rho)_{CNC}}{w_{CNC}[(\mu/\rho)_{CNC} - (\mu/\rho)_{ALG}] + 100(\mu/\rho)_{ALG}} \quad (4)$$

was used to described the dependence of the intensity against cellulose load. Here I_{200} refers to the intensity of the (2,0,0) reflection, I_{200}^{0} refers to the intensity of the (2,0,0) reflection of a pure cellulose fiber, w represents CNC load in wt %, μ is the linear absorption coefficient, ρ is the density, the ratio μ/ρ is the mass absorption coefficient, and the subindexes CNC and ALG refer to cellulose nanocrystals and calcium alginate, respectively. Equation 4 was originally derived for a symmetrical reflection geometry;[26] however, it remains valid for the normal-beam transmission system employed in this study as long as μt remains approximately constant for every sample, where t is the thickness of the specimen. The value of μ can be experimentally determined by measuring the intensity of the direct beam after traveling through a specimen of known thickness.

The intensity versus concentration calibration curve in Figure 9 shows an exceptionally good correlation between experimental data and the fitted curve, as evidenced by the R^2. However, caution should be employed when using this curve. The Ca^{2+} ions present in the alginate matrix and on the surface of the nanoparticles as well as the sulfur atoms accompanying the CNC are very strong X-ray absorbents compared to carbon and oxygen. A small variation in the concentration of those elements can affect the mass absorption coefficient of the individual phases and thus change the values of the regression parameters. A curve like the one depicted in Figure 9 should not be employed if the

elemental composition of each phase is not constant for all samples. Another precaution must be taken when dealing with oriented samples. Since the intensity is dependent on azimuthal angle, it is then necessary to "randomize" it by calculating an integrated intensity over the entire angular range; this was done in Figure 5. Regardless, WAXD provides a reliable nondestructive method to measure the concentration of a crystalline phase in a solid matrix, which would be very difficult to achieve with other techniques.

CONCLUSIONS

WAXD was used to study the effect of CNC on the structure of calcium alginate fibers and to correlate those effects to the mechanical properties measured in our recent paper.[1] The junction zones of the calcium alginate mainly consisted on MG dimers with a repeat distance of 0.91 nm; this structure was present regardless of nanofiller load and processing conditions. A slight increase in alginate crystallinity was observed upon addition of the CNC; however, it did not explain the reduction of tenacity and modulus at constant J_A. On the other hand, the degree of orientation of the cellulose crystallites was found to decrease as the load increased, since the CNC interparticle interactions induced twisting away from the drawing direction. At high enough concentrations and sufficiently low jet stretches, the crystallites within the alginate matrix assembled in a spiral orientation around the fiber longitudinal axis, similarly to native cellulose fibers. The appearance of the spiral coincided with a reduction in the nanocomposite tenacity and modulus. WAXD was also used as a nondestructive technique to measure the concentration of the crystalline filler inside the fibers. It was demonstrated that a simple variation in processing conditions can be used to tune the mechanical properties of cellulose-based nanocomposites, which directly correlate with CNC orientation. Moreover, we demonstrated the ability to produce CNC polymer nanocomposites with improved toughness without significantly compromising the strength.

AUTHOR INFORMATION

Corresponding Author

*Phone: (864) 656-2131. E-mail: ckitche@clemson.edu.

ACKNOWLEDGMENT

The authors thank the Center for Advanced Engineering Fibers and Films at Clemson University for support, the Graduate School at Clemson University for PSA-NGGF fellowship, and Marlon Morales for his valuable collaboration with WAXD measurements.

REFERENCES

(1) Ureña-Benavides, E. E.; Brown, P. J.; Kitchens, C. L. *Langmuir* **2010**, *26*, 14263–14270.
(2) Hassan, M.; Abou-Hussein, R.; Zhang, X.; Mark, J.; Noda, I. *Mol. Cryst. Liq. Cryst.* **2006**, *447*, 23–44.
(3) Takahashi, T.; Yonetake, K.; Koyama, K.; Kikuchi, T. *Macromol. Rapid Commun.* **2003**, *24*, 763–767.
(4) Eichhorn, S. J.; Baillie, C. A.; Zafeiropoulos, N.; Mwaikambo, L. Y.; Ansell, M. P.; Dufresne, A.; Entwistle, K. M.; Herrera-Franco, P. J.; Escamilla, G. C.; Groom, L.; Hughes, M.; Hill, C.; Rials, T. G.; Wild, P. M. *J. Mater. Sci.* **2001**, *36*, 2107–2131.
(5) Klemm, D.; Heublein, B.; Fink, H.-P.; Bohn, A. *Angew. Chem., Int. Ed.* **2005**, *44*, 3358–3393.
(6) Habibi, Y.; Lucia, L. A.; Rojas, O. J. *Chem. Rev.* **2010**, *110*, 3479–3500.
(7) Dufresne, A. *Can. J. Chem.* **2008**, *86*, 484–494.
(8) Azizi Samir, M. A. S.; Alloin, F.; Dufresne, A. *Biomacromolecules* **2005**, *6*, 612–626.
(9) Anglès, M. N.; Dufresne, A. *Macromolecules* **2001**, *34*, 2921–2931.
(10) Grunert, M.; Winter, W. T. *J. Polym. Environ.* **2002**, *10*, 27–30.
(11) Qin, Y. *Polym. Int.* **2008**, *57*, 171–180.
(12) Ertesvåg, H.; Valla, S. *Polym. Degrad. Stab.* **1998**, *59*, 85–91.
(13) Gacesa, P. *Carbohydr. Polym.* **1988**, *8*, 161–182.
(14) Rånby, B. G. *Discuss. Faraday Soc.* **1951**, *11*, 158–164.
(15) Revol, J.-F.; Godbout, L.; Dong, X.-M.; Gray, D. G.; Chanzy, H.; Maret, G. *Liq. Cryst.* **1994**, *16*, 127–134.
(16) Gray, D. G. *Cellulose* **2008**, *15*, 297–301.
(17) Fraser, R. D. B.; Macrae, T. P.; Miller, A.; Rowlands, R. J. *J. Appl. Crystallogr.* **1976**, *9*, 81–94.
(18) Nishiyama, Y.; Langan, P.; Chanzy, H. *J. Am. Chem. Soc.* **2002**, *124*, 9074–9082.
(19) Alexander, L. E. In *X-Ray Diffraction Methods in Polymer Science*; Robert, E., Ed.; Krieger Publishing Co.: Huntington, NY, 1979; pp 198–277.
(20) Donati, I.; Holtan, S.; Mørch, Y. A.; Borgogna, M.; Dentini, M.; Skjåk-Bræk, G. *Biomacromolecules* **2005**, *6*, 1031–1040.
(21) Sikorski, P.; Mo, F.; Skjåk-Bræk, G.; Stokke, B. T. *Biomacromolecules* **2007**, *8*, 2098–2103.
(22) Favier, V.; Canova, G. R.; Shrivastava, S. C.; Cavaillé, J. Y. *Polym. Eng. Sci.* **1997**, *37*, 1732–9.
(23) Sisson, W. A. *Ind. Eng. Chem* **1935**, *27*, 51–56.
(24) DeLuca, L. B.; Orr, R. S. *J. Polym. Sci.* **1961**, *54*, 457–470.
(25) Elazzouzi-Hafraoui, S.; Nishiyama, Y.; Putaux, J.; Heux, L.; Dubreuil, F.; Rochas, C. *Biomacromolecules* **2008**, *9*, 57–65.
(26) Klug, H. P.; Alexander, L. E. In *X-Ray Diffraction Procedures: For Polycrystalline and Amorphous Materials*, 2nd ed.; John Wiley & Sons: New York, 1974; pp 505–565.